

TROPICAL METEOROLOGY

Intertropical Convergence Zone

D E Waliser, State University of New York, Stony Brook, NY, USA

Copyright 2002 Elsevier Science Ltd. All Rights Reserved.

doi:10.1006/rwas.2002.0417

Waliser, D E

State University of New York,
Institute for Terrestrial and Planetary Atmospheres,
Endeavour Hall, Room 205,
Stony Brook, NY 11794, USA

Introduction

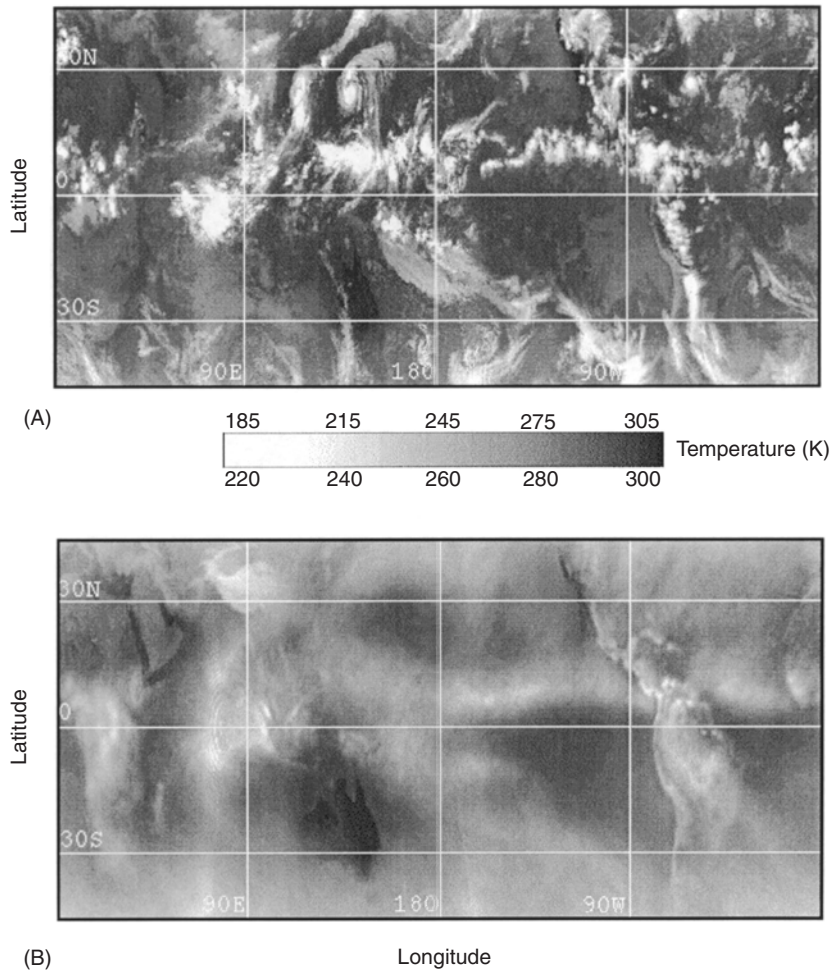
0417-P0005 One of the features that is most readily identified with the tropical atmosphere is the Intertropical Convergence Zone (ITCZ). The ITCZ lies in the equatorial trough, a permanent low-pressure feature that marks the meteorological Equator where surface trade winds, laden with heat and moisture from surface evaporation and sensible heating, converge to form a zone of increased mean convection, cloudiness, and precipitation. The latent heat released in the convective cloud systems of the ITCZ is a critical component of the atmospheric energy balance, and the enhanced cloudiness associated with these cloud systems provides an important contribution to the planetary albedo. The fluxes of heat, moisture, momentum, and radiation between the atmosphere and the surface differ dramatically between the ITCZ region and the regions to the north and south of the ITCZ. Thus the position, structure, and migration of the ITCZ play an important role in determining the characteristics of ocean–atmosphere and land–atmosphere interactions on a local scale, the circulation of the tropical oceans on a basin scale, and a number of features of the Earth’s climate on a global scale.

Mean Structure

0417-P0010 On any given day in the tropics, there are usually a number of deep convective cloud systems that appear to be somewhat randomly distributed across the equatorial region. **Figure 1A** shows a satellite cloud image constructed from a number of geostationary and polar orbiting satellites for 7 September 1991. Bright areas denote cold temperatures, and thus in this

case indicate clouds whose tops are at or near the level of the tropopause, e.g., deep convective or cirrus clouds. Dark areas denote warm temperatures, which in this case implies clear skies. Evident throughout the tropical region, and aligned roughly parallel to the Equator, are a number of cloud systems. Some of these systems exhibit horizontal scales on the order of a few hundred kilometers or less. Others, such as the large system in the Indian Ocean, have horizontal dimensions on the order of about 25 000 km. The vast difference in horizontal scales of these cloud systems can arise from a number of factors. Typically, the more mature a convective system is, the larger its horizontal extent. This is mostly due to the development of high cirrus clouds in the outflow region of convective systems. In contrast to deep convective “towers”, which typically have horizontal scales on the order of 1–10 km and when found in isolation usually indicate young or developing convective systems, cirrus clouds can appear to extend over thousands of kilometers and encompass tens or hundreds of convective towers simultaneously. Thus the sizes of the various convective systems shown in **Figure 1A** can be influenced by their maturity and their abundance in any one area, and how these factors in turn influence the development of what appears as a common cirrus cloud. Further, while most cloud systems in the tropics arise from simple convective instability, probably in conjunction with synoptic wavelike disturbances inherent to the equatorial region, the organization of some systems can be influenced by low-frequency phenomena that can increase their spatial extent. For example, the larger systems in the Indian and western Pacific Ocean may be influenced by the tropical Intraseasonal Oscillation or simply be larger owing to the difference in climatological conditions (e.g., sea surface temperature) between the Eastern and Western hemispheres, which is discussed below.

Other than the loose east–west orientation of the cloud systems in **Figure 1A**, there is no obvious systematic preference for the locations of these systems. Only upon averaging such observations over a time that is relatively long (order of months) compared to the lifetimes of these systems (order of hours–days) does a robust spatial preference become evident. **Figure 1B** shows a time-averaged satellite cloud image, constructed from daily cloud images such as the one shown in **Figure 1A**, from 1 September to 31 November 1991. From this image, it is more apparent that for a given season particular regions of the tropics are favored for the development of tropical

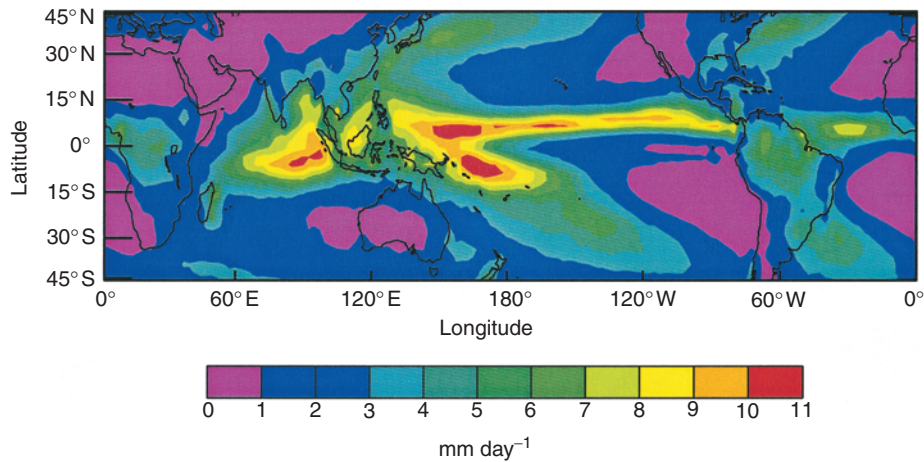


0417-F0001 **Figure 1** Cloud images constructed from $11\ \mu\text{m}$ radiances measured from a number of geostationary and polar-orbiting weather satellites. (A) Instantaneous cloud field for 00 GMT 7 September 1991. (B) Time-mean 00 GMT cloud field for September through November 1991. Radiance values have been converted to equivalent blackbody temperature using the Stefan–Boltzmann law. (Global Cloud Imagery courtesy of M. Salby, University of Colorado.)

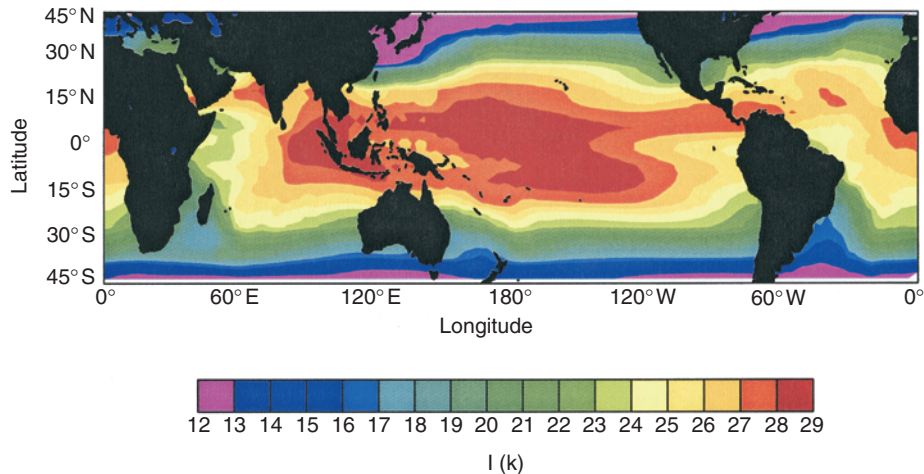
convective systems. The spatial structure of the deep convective cloud pattern shown in **Figure 1B** exhibits the spatial pattern roughly identified with the ITCZ, at least for the Northern Hemisphere fall season. Thus while the cloud (or rainfall) pattern associated with the ITCZ is usually thought of as a continuous band of clouds (or rain), at any given time this “band” contains only a few disparate cloud systems. **Figure 2** shows the long-term mean rainfall pattern. The band(s) of high rainfall represent the mean, or archetypal, ITCZ spatial structure. Overall, this structure is roughly aligned with the Equator and it exhibits a significant amount of zonal symmetry relative to the rainfall pattern in the mid-latitudes. Apart from this zonal symmetry, the ITCZ rainfall distribution displays a fair amount of longitudinal variability as well. In the Atlantic and eastern Pacific Oceans, it is made up of very narrow, intense regions of rainfall that tend to lie

just north of the Equator. Over the South American and African continents, the mean rainfall distribution has a considerably larger latitudinal extent and tends to lie directly over the Equator. Over the eastern Indian and western Pacific Oceans, the rainfall distribution is both broad in latitude and intense in magnitude. Two of the more notable zonal asymmetries in the ITCZ are the weak rainfall over the western Indian Ocean and the south-east extension of the ITCZ over the central Pacific Ocean. The latter, referred to as the South Pacific Convergence Zone (SPCZ), leads to an area of intense rainfall on either side of the Equator with a relatively dry region in between. Such a structure is often referred to as a “double ITCZ.”

The time-mean spatial structure of the ITCZ 0417-P0020 described above can be better understood by examining the time-mean sea surface temperature (SST), which is shown in **Figure 3**. Because on average the



0417-F0002 **Figure 2** Long-term mean (1979–1996) rainfall rate constructed from a combination of satellite-derived products and in situ observations. (Source: National Oceanographic and Atmospheric Administration's (NOAA) Climate Prediction Center (CPC) Merged Analysis of Precipitation (CMAP).)

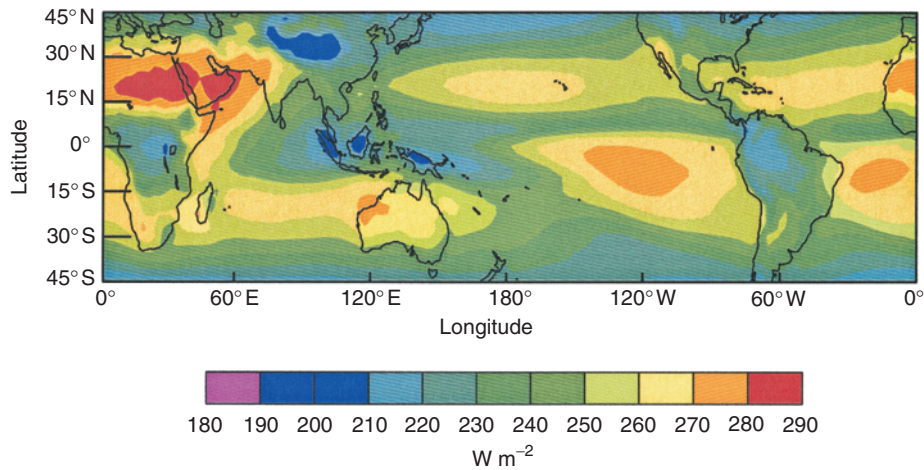


0417-F0003 **Figure 3** Long-term mean (1968–1996) sea surface temperature constructed from a combination of satellite-derived values and in situ observations. (Source: NOAA's National Environmental Satellite, Data, and Information Service.)

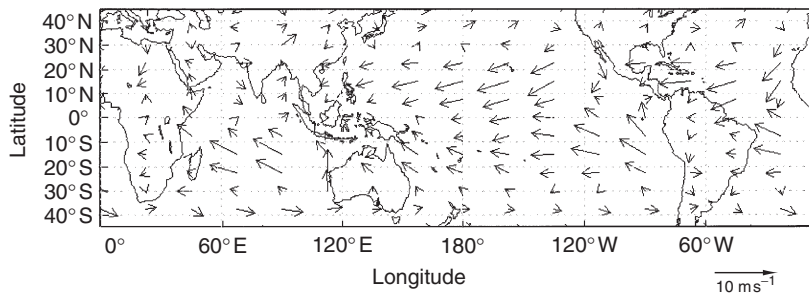
equatorial region receives the most solar irradiance, this region also tends to have the highest SSTs. While this tendency for very warm SST (i.e., greater than 25°C) is mostly uniform with longitude, there are some deviations. These deviations are produced by a number of factors, including ocean basin geometry, ocean circulation properties (equatorial dynamics in particular) and the coupled interaction with the atmosphere, including the ITCZ itself. The relatively warm water of the equatorial region heats the air in the lower atmosphere, making it less dense and more buoyant relative to the air aloft. This buoyancy forcing leads to rising motion over the equatorial region. As the moist near-surface air rises, it cools adiabatically and begins to undergo condensation, which releases the latent heat contained in the water vapor and

produces rainfall at the surface. This latent heating enhances the buoyancy and associated upward motion of the air even further, which in turn enhances the adiabatic cooling, water vapor condensation, and surface rainfall. This process continues until nearly all the water vapor condenses out of the parcel and/or the parcel is no longer buoyant with respect to its environment. In either case, this usually happens when the parcel reaches the inversion associated with the tropopause, whereupon the air begins to move away from the Equator. This divergent upper-level air undergoes cooling through radiative heat loss, which causes it to lose buoyancy, and sinks in the subtropical regions.

Figure 4 shows the long-term mean outgoing thermal radiation leaving the top of the atmosphere. 0417-P0025



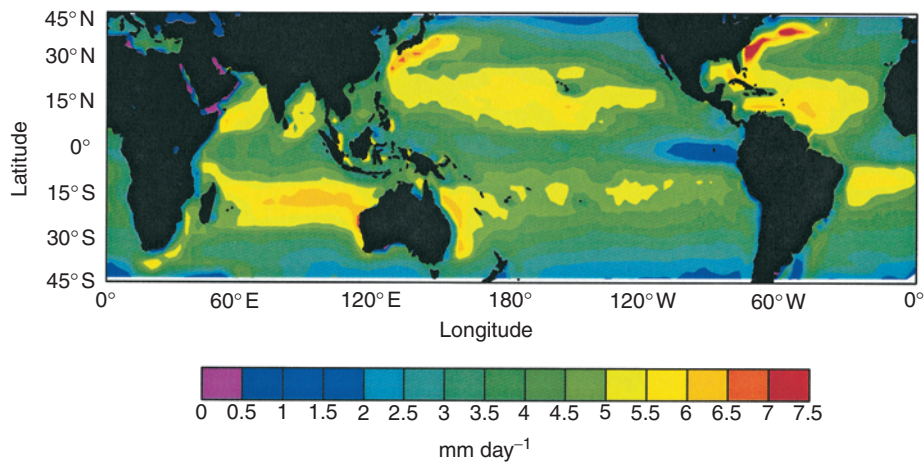
0417-F0004 **Figure 4** Long-term mean (1974–1998) satellite-derived outgoing thermal radiation. (Source: NOAA's National Environmental Satellite, Data, and Information Service.)



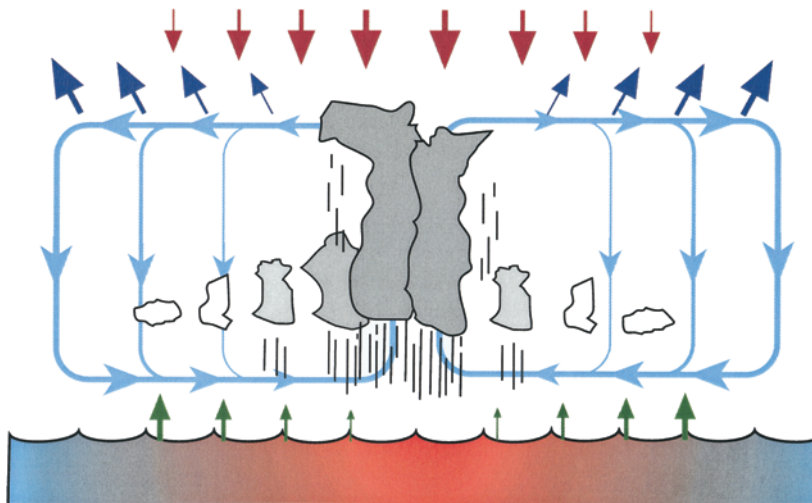
0417-F0005 **Figure 5** Long-term mean (1968–1996) surface wind values derived from a combination of in situ observations and analyses using a numerical weather prediction model. (Source: National Centers for Environmental Prediction/National Center for Atmospheric Research Reanalysis Project.)

The regions of large radiative heat loss lie on the poleward edges of the regions of high rainfall (Figure 2) and extend into the subtropics. Upon reaching the surface, this sinking air is relatively dry but gains moisture again via surface evaporation as it converges towards the Equator. Figures 5 and 6 show the long-term mean surface wind and evaporation fields. The surface wind field shows that over most of the tropical regions surface air tends to converge into the areas of high rainfall. The evaporation field indicates that as this air converges toward these equatorial regions, it gains moisture from the ocean, particularly in the areas of the trade winds where the wind speeds are higher. The combination of the above processes leads to a deep meridional circulation cell, extending over the depth of the troposphere, with air converging toward the Equator at low levels, rising in the equatorial regions, diverging at upper levels, and sinking in the subtropics. The zonal mean of this circulation pattern is typically referred to as the “Hadley circulation.”

From the physical description above, it is evident that a close association exists between the spatial structure of the warmer SSTs and the rainfall pattern associated with the ITCZ. For example, Figures 2 and 3 show that the narrow bands of rainfall over the Atlantic and eastern Pacific correspond well to the relatively warm bands of warm water north of the Equator in these regions. Similarly, the very broad area of warm water in the Indian and western Pacific Ocean corresponds well to the more widespread area of intense rainfall of the ITCZ in these regions. In addition, the discussion above highlights the complex makeup of the water and energy cycles in the tropics and the role of the ITCZ within these cycles. The schematic diagram in Figure 7 highlights important aspects of these water and energy cycles and illustrates how the physical processes associated with the ITCZ described above fit together in an idealized latitude–height diagram. The downward arrows at the top of the atmosphere depict the incoming solar energy from the sun and the fact that there is a reduction of solar



0417-F0006 **Figure 6** Long-term mean (1968–1996) ocean surface evaporation values constructed from a combination of in situ values and analyses using a numerical weather prediction model. (Source: National Centers for Environmental Prediction/National Center for Atmospheric Research (NCEP/NCAR) Reanalysis Project.)



0417-F0007 **Figure 7** Schematic depiction of the ITCZ in the context of the water and energy cycles of the tropics. The downward arrows at the top of the atmosphere depict the incoming solar energy from the Sun. The upward arrows leaving the surface of the ocean depict the transfer of heat and moisture from the ocean to the near-surface air via sensible heat and latent (i.e., evaporative) heat fluxes. The upward arrows at the top of the atmosphere denote this energy being transferred back to space via radiative heat loss.

energy as one moves poleward. As **Figure 1A** indicates, at any given time most of the tropics exhibits clear skies. This allows a large portion of this solar energy to reach the surface and induce a pole-to-equator SST gradient, with the warmest SSTs in the near-equatorial region. The upward arrows at the surface of the ocean depict the ocean-to-atmosphere energy exchange, which takes place primarily through the transfer of heat and moisture from the ocean to the near-surface air via sensible heat and latent (i.e., evaporative) heat fluxes. As the air rises over the warmest water, a convergent circulation is induced at lower levels, with

the upper levels exhibiting divergence. The rising air experiences adiabatic cooling, which leads to condensation of the moisture and the release of the stored latent heat. The former falls back to the surface as precipitation while the latter heats the air, leading to a further enhancement of the vertical motion. Now, the heat that was originally derived from incoming solar energy deposited in the ocean resides in the atmosphere. The upward arrows at the top of the atmosphere denote transfer of this energy back to space via radiative heat loss as the air diverges away from the Equator and sinks back to the surface.

Seasonal Variations

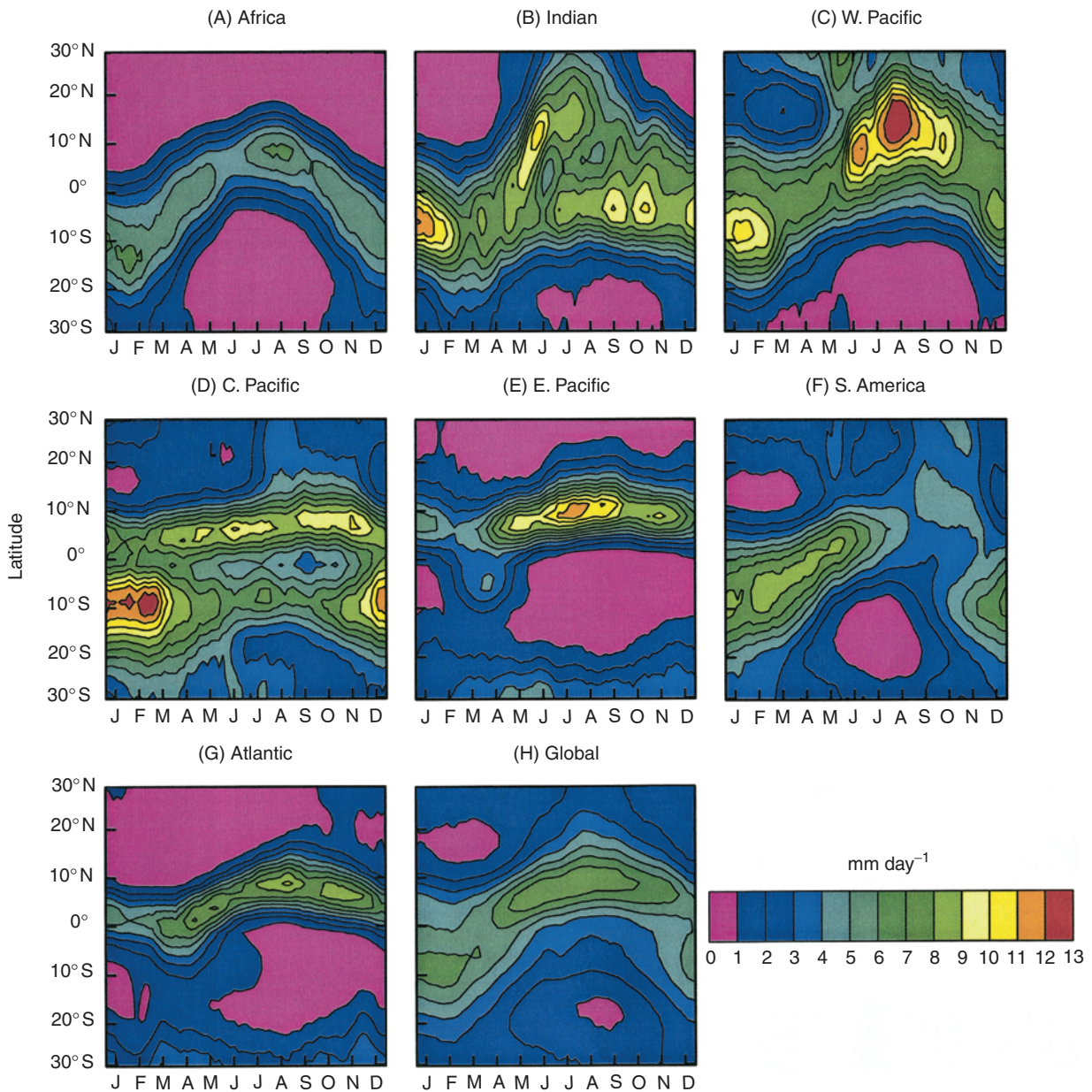
0417-P0035 Over the course of the annual cycle, seasonal changes occurring in the ITCZ modify the mean structure depicted in **Figure 2**. In general, the entire line-oriented convection band marches north in the Northern Hemisphere spring and summer, and south in the Southern Hemisphere spring and summer. The differences in the amplitudes and phases of the ITCZ excursions at different longitudes are dictated in part by the different characteristics of the surface (i.e., land or ocean) and the local atmospheric circulation pattern. The ITCZ over land (e.g., Africa and South America) follows the annual march of the Sun, while the migration of the ITCZ over extended ocean regions lags slightly behind by a month or two. This time lag is most apparent in the eastern Pacific and the Atlantic Oceans, where the ITCZ is farthest south in the Northern Hemisphere spring and farthest north in the Northern Hemisphere fall. The origin of this time lag is primarily the large thermal inertia of the ocean mixed-layer compared to that of the land surface but also involves complex dynamical interactions that develop between the ocean and atmosphere.

0417-P0040 While the most of the seasonal changes in the ITCZ are associated with latitudinal migration, there are other significant structural changes. One of the more significant of these is over South America where large spatial differences exist between the “ITCZs” of the Northern and Southern Hemisphere summers. During the Southern Hemisphere summer, the rainy season encompasses nearly the entire tropical area of the South American continent. This produces a latitudinally and longitudinally broad ITCZ. In the Northern Hemisphere summer, the ITCZ overlies the oceanic region north of the continent and has a structure more consistent with its oceanic counterparts to the east and west. Another dramatic seasonal change associated with the ITCZ occurs in the Indian Ocean region during the Asian summer monsoon. As the monsoon circulation develops and intensifies, the convection zone splits, with a very intense area of rainfall occurring over the Indian subcontinent and a weaker rainfall maximum remaining in the equatorial region. A similar intensification of rainfall occurs in the Southern Hemisphere summer over northern Australia; however in this case the equatorial component tends to be suppressed. During this same period, the convergence zones over Africa and the Indian Ocean become more continuous owing to the reduced coastal ocean upwelling off the east African coast. Other modest seasonal deviations occur in the eastern Pacific during the northern spring, when the ITCZ occasionally separates into two zones of convection straddling the Equator. This “double ITCZ” results from a

relaxation of the south-east trade winds, which greatly diminishes the equatorial and nearby coastal ocean upwelling, leaving seasonably warm surface temperatures south of the Equator. In a related manner, the two branches of convergence in the central Pacific oscillate in strength during the year with the southern and northern branches intensifying during their respective summer season.

To help illustrate and quantify some of the seasonal changes in the ITCZ described above, **Figure 8** shows time–latitude diagrams of rainfall over the course of the calendar year for a number of distinct tropical regimes. For example, **Figure 8A** shows that the annual cycle of the ITCZ over Africa exhibits a migration pattern that has a nearly sinusoidal nature. In this region, the ITCZ appears to closely follow the solar cycle of surface heating, with a lag of about a month. It has a fairly even intensity throughout the year ($\sim 5 \text{ mm day}^{-1}$) and migrates from about 15°S to 10°N . The difference in poleward extremes is associated with the Sahara Desert, the dryness of which inhibits the northern migration of the ITCZ. In contrast to this nearly sinusoidal case, all other regions (**Figures 8B–8G**) show an annual cycle that has seasonal dependences in intensity and structure, and/or a larger phase lag relative to the solar cycle of surface heating. For example, the ITCZ migrations over the Indian (**Figure 8B**) and western Pacific (**Figure 8C**) Oceans show strong rainfall intensification associated with the summer monsoons. In particular, the Asian summer monsoon produces a significant enhancement to the rainfall in the Northern Hemisphere summer months over south-east Asia and, as mentioned above, produces two bands of rainfall in the Indian Ocean region during this period. The annual cycle of the ITCZ in these two regions lags approximately 2 months behind the solar heating cycle.

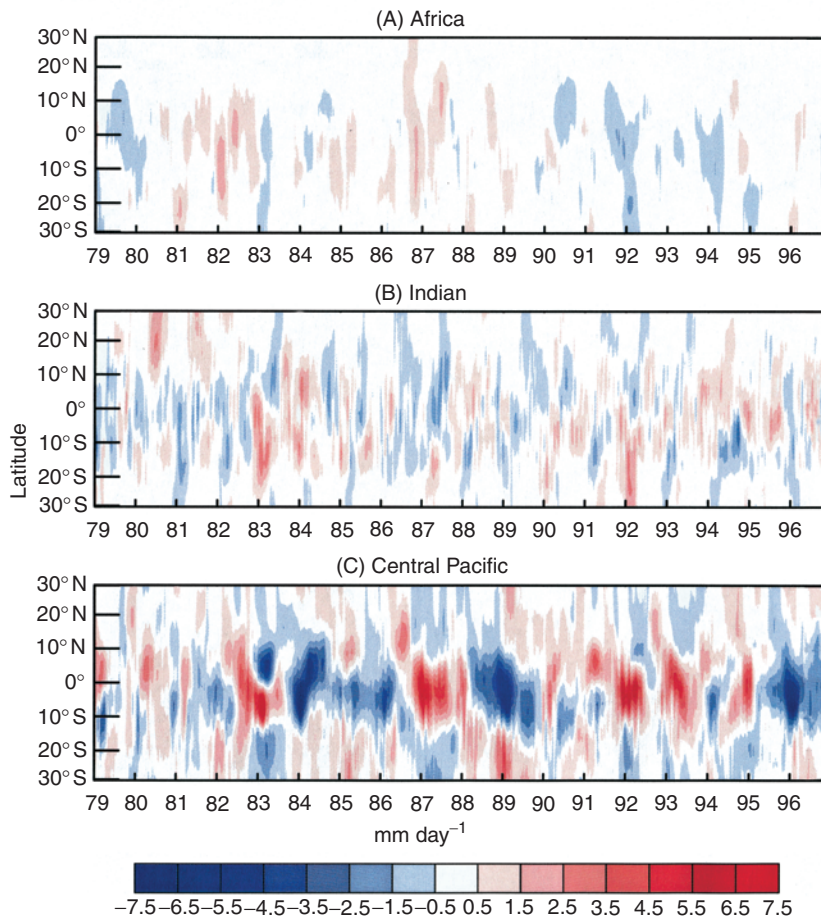
The eastern Pacific (**Figure 8E**) and Atlantic (**Figure 8G**) Oceans have very similar annual cycles. As suggested earlier by **Figures 1b** and **2**, the ITCZ in these regions remains primarily in the Northern Hemisphere throughout the year, with some weak rainfall ($\sim 4\text{--}5 \text{ mm day}^{-1}$) occurring south of the Equator in the Northern Hemisphere spring. During this time of year, warm water ($\sim 27^\circ \text{C}$ or higher) occurs on both sides of the Equator in this region and the ITCZ, in its southernmost position, is split by a zone equatorial ocean upwelling (i.e., cool equatorial SSTs). The phase of the annual cycle in these regions lags behind the surface solar heating cycle by approximately 2–3 months, and each produces the most intense ITCZ in the Northern Hemisphere fall. During this season, the surface water associated with the equatorial countercurrents is warmest and the low-level trade wind convergence is strongest.



0417-F0008 **Figure 8** Time–latitude diagrams of the annual cycle of the ITCZ, in terms of rainfall, zonally averaged over eight different longitude sectors. (A) Africa, 10–40° E; (B) Indian, 60–100° E; (C) western Pacific, 110–150° E; (D) central Pacific, 160° E–160° W; (E) eastern Pacific, 100–140° W; (F) South America, 45–75° W; (G) Atlantic, 10–40° W; (H) global, 0–360° E. Mean annual cycles were computed from the period 1979 to 1996. (Source: National Oceanographic and Atmospheric Administration’s (NOAA) Climate Prediction Center (CPC) Merged Analysis of Precipitation (CMAP).)

0417-P0055 The annual cycle of the central Pacific and South America show very different characteristics from those described above. As illustrated earlier in **Figure 2**, the ITCZ in the central Pacific is composed of northern and southern convergence zones straddling the Equator. While this large-scale “double” convergence zone remains intact during the course of the annual cycle, the intensity of the summer hemisphere branch tends to dominate. The annual cycle of the

ITCZ over South America displays the least amount of symmetry with respect to north–south migration and ITCZ intensity. The surface underlying the ITCZ is largely responsible for this asymmetry, as mentioned above. In this region, the phase of the ITCZ is locked to the annual cycle during its northward propagation. However, after having reached the oceanic region north of South America, the convection diminishes slightly, and the cycle appears to lag slightly until the



0417-F0009 **Figure 9** Time–latitude diagrams of the anomalies in rainfall associated with the ITCZ zonally averaged over three different longitude sectors: (A) Africa, 10–40° E; (B) Indian, 60–100° E; and (C) central Pacific, 160° E–160° W. Departures are computed from the mean annual cycles shown in **Figure 8**. (Source: National Oceanographic and Atmospheric Administration’s (NOAA) Climate Prediction Center (CPC) Merged Analysis of Precipitation (CMAP).)

rainy season begins again over the Amazon Basin in November–December. The annual cycle of the global ITCZ has a modest resemblance to a sinusoidal pattern, with the intensity of the zonally averaged mean rainfall being strongest during the Northern Hemisphere summer and fall ($\sim 7 \text{ mm day}^{-1}$), and weakest during the equinoxes ($\sim 5 \text{ mm day}^{-1}$).

Interannual Fluctuations

0417-P0060 Apart from the regular seasonal variations, the ITCZ undergoes interannual fluctuations in its position and intensity. **Figure 9** illustrates the range of interannual variability exhibited by the ITCZ over the period 1979 to 1998 for three of the longitude sectors discussed in the previous section. This figure shows time–latitude diagrams of the seasonal anomalies of rainfall from the mean annual cycles presented in **Figure 8**. Note that each is plotted using the same color scale. Immediately

evident is the fact that the interannual anomalies in the ITCZ position and intensity are weakest over Africa and strongest for the ITCZ over the central Pacific Ocean. Typical seasonal rainfall anomalies for the ITCZ over Africa are about $\pm 0.5 \text{ mm day}^{-1}$ and range up to about $\pm 1.5 \text{ mm day}^{-1}$ in the more extreme events. Depending on the location and intensity of the mean ITCZ rainfall band, these values represent variations on the order of 10–25% of the mean values. Overall these anomalies illustrate that this region undergoes relatively weak, low-frequency rainfall variations, with the early and late 1980s being relatively wetter than normal and the late 1970s and early 1990s being relatively drier than normal. Within this low-frequency variability are periods when the ITCZ exhibits short-lived variability in its intensity and latitude. For example, during the 1981–1982 winter the ITCZ extended anomalously southward, while in the 1982–1983 winter the rainfall associated with the ITCZ was about 25% stronger than normal.

During the fall of 1986 and summer of 1987, the ITCZ extended anomalously northward, bringing rain to the normally dry Sahara Desert. Another notable anomaly in the ITCZ over Africa occurred in the winter of 1991–1992 when the ITCZ was particularly weak and did not migrate as far south as normal.

0417-P0065 The time–latitude rainfall anomaly diagram for the Indian Ocean region (**Figure 9B**) shows variability quite different than that exhibited by the ITCZ over Africa. First, the meridional extent of the anomalous excursions is much greater, extending to at least 30° . For the most part, this is simply related to the much broader latitudinal extent of the mean ITCZ pattern in this region (i.e., **Figures 2** and **8**). Second, the intensity of the fluctuations is slightly greater, ranging up to about $\pm 3 \text{ mm day}^{-1}$. However, given the larger mean rainfall values for this region, this anomaly range represents deviations from the annual cycle on the order of 25%, which is similar to the case for Africa. Third, even with the seasonal smoothing applied to the data, the ITCZ in this region exhibits considerably more variability at shorter time scales than, for example, the ITCZ over Africa. This shorter-term variability is partly attributable to the Intraseasonal Oscillation that has been found to prevail most strongly over the Indian and western Pacific Oceans. Given the distribution of land and people within this sector, the most consequential of the rainfall anomalies occur in the Northern Hemisphere summer, north of about 15°N . From **Figure 7**, it can be seen that the maximum rainfall associated with the Indian summer monsoon occurs in July. **Figure 8B** illustrates some aspects of the variability associated with the timing and strength of the Asian monsoon as it relates to the ITCZ. For example, in 1980, the rainfall associated with the northward migration of the ITCZ and the development of the summer monsoon was particularly intense, while the 1981 summer monsoon appears to have come slightly earlier than normal. In contrast, the summer monsoons of 1983, 1987, and 1989 are examples of the monsoon-related ITCZ rainfall being a little weaker than normal. It is important to emphasize that even though these anomalies ($\sim 1 \text{ mm day}^{-1}$) represent only about 10% of the total rainfall that typically occurs during the monsoon (**Figure 8B**), they represent very important departures for the people and industries (e.g., agriculture) that are affected by them.

0417-P0070 For the case of the central Pacific (**Figure 9C**), the anomalous ITCZ rainfall is dominated by negative and positive anomalies on or near the Equator. Note that these values are significantly larger than the ITCZ rainfall anomalies occurring in either of the other longitude sectors discussed above (and in those longitude sectors not discussed). In this region, the zonally

averaged rainfall anomalies range up to at least $\pm 7 \text{ mm day}^{-1}$. In some instances, particularly for the large anomalies right on the Equator, these values can exceed 100% of the mean values associated with the annual cycle (**Figure 7D**). These large variations in the position and intensity of the ITCZ in this region are associated with climate phenomena known as the El Niño–Southern Oscillation (ENSO). In warm phases of ENSO (i.e., El Niño), SST in the central and eastern equatorial Pacific Ocean can become anomalously warm by about $1\text{--}3^\circ \text{C}$, while in cold phases (i.e., La Niña) this region becomes anomalously cool by a similar magnitude. This has a dramatic effect on the organization of tropical convection in this region as well as in regions remote from the central Pacific. Evident from **Figure 9C** are the large positive rainfall anomalies associated with the strong El Niño of 1982–1983, the moderate El Niño of 1986–1987, and the prolonged and somewhat weaker El Niño(s) of the early 1990s. Typically, these events cause the two convergence zones that are located slightly away from the Equator in the central Pacific to merge into a single zone of convection and rainfall centered on or very near the Equator. The large negative equatorial rainfall anomalies are associated with the La Niñas of 1984, 1988–1989, and 1995–1996. Central Pacific rainfall anomalies associated with La Niña typically cause the relatively dry equatorial zone near the dateline (**Figure 2**) to become even drier and to extend farther west than normal. It is important to point out that these central Pacific ENSO-related ITCZ rainfall anomalies do not occur in isolation. Typically, these anomalies induce anomalies of the opposite sense and a somewhat weaker magnitude in the western Pacific sector, and in some cases the Indian Ocean and South American sectors as well. In fact, these ENSO-related rainfall anomalies are so large that they are the only significant departure that appears to occur in the global mean ITCZ (not shown). Anomalies in the global mean ITCZ rainfall are typically in phase with the anomalies in the central and eastern Pacific Ocean and have magnitudes that range up to about 1 mm day^{-1} . However, with respect to quantifying the size of this climate signal in the context of the ITCZ, it is important to point out that accurate measurements of rainfall over the oceanic regions is possible only with satellite retrievals and this is still an area of active research.

See also

Tropical Meteorology: Equatorial Waves (0414); Intraseasonal Oscillation (Madden-Julian Oscillation) (0415); Tropical Climates (0416).

Further Reading

- Emanuel KA (1994) *Atmospheric Convection*. New York: Oxford University Press.
- Gill AE (1982) *Atmosphere–Ocean Dynamics*. Orlando: Academic Press.
- Henderson-Sellers A and Robinson PJ (1986) *Contemporary Climatology*. Harlow: Longman Scientific and Technical.
- Houghton JT (1986) *The Physics of the Atmosphere*. Cambridge: Cambridge University Press.
- Kidder SQ and Vonder Haar TH (1995) *Satellite Meteorology: An Introduction*. San Diego: Academic Press.
- Kraus EB and Businger JA (1994) *Atmosphere–Ocean Interaction*. New York: Oxford University Press.
- Lindzen RS (1990) *Dynamics in Atmospheric Physics*. Cambridge: Cambridge University Press.
- Salby ML (1996) *Fundamentals of Atmospheric Physics*. San Diego, CA: Academic Press.